HHS Public Access

Author manuscript

J Tissue Eng Regen Med. Author manuscript; available in PMC 2019 March 01.

Published in final edited form as:

J Tissue Eng Regen Med. 2018 March ; 12(3): e1325–e1336. doi:10.1002/term.2512.

Prevascularization of Natural Nanofibrous Extracellular Matrix for Engineering Completely Biological 3D Prevascularized Tissues for Diverse Applications

Lijun Zhang[1,2,#], **Zichen Qian**[2,#], **Mitchell Tahtinen**[2], **Shaohai Qi**[1,*], and **Feng Zhao**[2,*]

[1]Department of Burns, the First Affiliated Hospital of Sun Yat-sen University, Guangzhou, Guangdong, China

[2]Department of Biomedical Engineering, Michigan Technological University, Houghton, Michigan, USA

Abstract

Self-sustainability after implantation is one of the critical obstacles facing large engineered tissues. A preformed functional vascular network provides an effective solution for solving the mass transportation problem. With the support of mural cells, endothelial cells (ECs) can form microvessels within engineered tissues. As an important mural cell, human mesenchymal stem cells (hMSCs) not only stabilize the engineered microvessel network, but also preserve their multi-potency when grown under optimal culture conditions. A prevascularized hMSC/ECM sheet fabricated by the combination of hMSCs, ECs and a naturally derived nanofibrous extracellular matrix (ECM) scaffold offers great opportunity for engineering mechanically strong and completely biological 3D prevascularized tissues. The objective of this study was to create a prevascularized hMSC/ECM sheet by co-culturing ECs and hMSCs on a nanofibrous ECM scaffold. Physiologically low oxygen (2% O_2) was introduced during the 7-day hMSC culture to preserve the stemness of hMSCs and thereby their capability to secrete angiogenic factors. The ECs were then included to form microvessels under normal oxygen (20% O_2) for up to 7 days. Results showed that a branched and mature vascular network was formed in the co-culture condition. Angiogenic factors VEGF, bFGF, and Ang-1 were significantly increased by low-oxygen culture of hMSCs, which further stabilized and supported the maturation of microvessels. Differentiation assay of the prevascularized ECM scaffold demonstrated a retained hMSC multi-potency in the hypoxia cultured samples. The prevascularized hMSC/ECM sheet holds great promise for engineering 3D prevascularized tissues for diverse applications.

Keywords

Microvessel; Prevascularization; Extracellular matrix scaffold; Mesenchymal stem cell; Angiogenesis; Nanofibrous scaffold

[*]Corresponding to: Feng Zhao, Department of Biomedical Engineering, Michigan Technological University, 1400 Townsend Drive, Houghton, MI 49931, U.S., Tel: 906-487-2852, Fax: 906-487-1717, fengzhao@mtu.edu. Shaohai Qi, Department of Burns, The First Affiliated Hospital of Sun Yat-sen University, Guangzhou, 510080, P. R. China, qishaohaigzburns@163.com.

[#]Equal contribution

1. Introduction

Successful tissue engineering strategies should restore the original biological function of tissues that are damaged or injured. Many tissue engineered constructs often fail due to insufficient supply of nutrients and oxygen, which has a maximum diffusion distance of approximately 200 μm from the adjacent vasculature (Lovett et al., 2009; Mercado-Pagán et al., 2015; Sakaguchi et al., 2015). To facilitate mass transportation, multiple strategies have been developed to create vascular networks within the engineered construct prior to implantation, including incorporation of growth factors to promote angiogenesis (Barati et al., 2016), pre-fabricated channels within synthetic scaffolds (Radisic et al., 2006), and co-culture of endothelial cells (ECs) with supporting cells (Wenger et al., 2004). Among these prevascularization strategies, the co-culture approach is the most biomimetic option, which can be achieved by growing ECs with mural cells, such as mesenchymal stem cells (MSCs) (Aguirre et al., 2010), fibroblasts (Czajka & Drake, 2015), or smooth muscle cells (SMCs) (Sakamoto et al., 2011).

Fibroblasts are one of the common cell types that have been used to support vascularization. Fibroblasts have been shown to secrete angiogenic factors, including vascular endothelial growth factor (VEGF), basic fibroblast growth factor (bFGF), transforming growth factor beta 1 (TGF-β1), along with matrix metalloproteinases (MMPs), to assist the sprouting, stabilization, and maturation of a vascular network formed by ECs (Czajka & Drake, 2015; Tunyogi-Csapo et al., 2007). Moreover, fibroblasts produce large quantities of extracellular matrix (ECM) components such as collagen, fibronectin and proteoglycans, to enhance the mechanical strength of the construct (Xing et al., 2014). However, subsequent research showed that fibroblasts from different sources vary in their supporting role for neovasculature formation. For example, the papillary dermis fibroblasts support angiogenesis, while reticular dermis fibroblasts do not, possibly due to differences in ECM composition and/or the incorporation of receptor-mediated signaling molecules secreted by these fibroblast subpopulations (Sorrell et al., 2008). Some fibroblasts, such as neonatal dermal fibroblasts and human pluripotent stem cell-derived fibroblasts, facilitate angiogenesis both *in vitro* and *in vivo* (Guerreiro et al., 2014; Shamis et al., 2013). However, as terminally differentiated cells, they are deficient in directly assisting tissue regeneration at implantation sites.

Compared to fibroblasts, MSCs have great potential to enhance angiogenesis while providing excellent regeneration stimulation. Implantation of MSCs and ECs co-cultured cell sheets has been shown to promote robust vascularization *in vivo* (Ren et al., 2014). Several groups created vascular networks on coverslips (Jinling et al., 2014), cell sheet constructs (Costa et al., 2016), and gelatin based hydrogels (Chen et al., 2012) by co-culturing MSCs and ECs, to demonstrate the angiogenic enhancement and translational potential of this strategy. Unfortunately, the resulting vascular network density was significantly lower than capillaries in native tissues. Other limitations include poor mechanical properties, for instance in gelatin scaffolds developed for bone tissue engineering (Chen et al., 2012). The low mechanical strength creates a requirement for additional scaffold material for translational applications (Costa et al., 2016), which exacerbates the mass transport problem. We have previously fabricated a vascularized

human MSC (hMSC) tissue by growing ECs on top of the hMSC sheet (Zhang et al., 2016). Nevertheless, to meet the mechanical criteria for scaffolding, the duration of cultivation for this vascularized hMSCs sheet was extensively long (4 weeks), which partially sacrificed the stemness of the hMSCs due to their tendency to differentiate over time during expansion. Shortening the cultivation time of hMSCs will undoubtedly benefit their stemness preservation and thereby their regenerative and immunoregulatory properties.

To improve the mechanical strength of hMSC sheets while maintaining their stemness, we proposed to incorporate a mechanically stronger ECM scaffold. We have previously developed a completely biological nanofibrous ECM scaffold that is decellularized from human dermal fibroblast (hDF) cell sheets (Xing et al., 2014). This ECM scaffold offers improved mechanical properties and features a nanofibrous structure. Furthermore, by using a fibroblast-derived ECM scaffold, the cultivation time of hMSCs can be significantly reduced. Vascularization of the ECM scaffold, by co-culture of hMSCs with ECs, could provide feasible options for replacing or repairing damaged cardiac tissues, neural tissues, skin tissues, blood vessels, or many other tissues.

The objective of this study was to create a prevascularized ECM scaffold by culturing hMSCs on a nanofibrous decellularized hDF-derived ECM scaffold, followed by co-culturing ECs on the hMSCs. According to the optimal culture condition that was achieved from our previous study, physiologically low oxygen (2% O_2, hypoxia) was introduced for 7 days into the hMSC culture to enhance their secretion of angiogenic factors; ECs were then co-cultured with hMSCs on the scaffold under normal oxygen (20% O_2, normoxia) conditions for up to 7 days to allow for vascularization (Zhang et al., 2016). It was expected that ECs would form microvessels, while hMSCs functioned as pericytes to stabilize and support the microvessels. The two cell culture groups were named as follows, H-group: hypoxia cultured hMSCs co-cultured with ECs under normoxia; N-group: normoxia cultured hMSCs co-cultured with ECs under normoxia. Human umbilical vein endothelial cells (HUVECs), typical ECs that are commonly used as model cells in studies of microvessel assembly *in vitro*, were selected to examine the prevascularization process of the ECM sheet. Angiogenic factors including VEGF and its receptor (VEGFR2), bFGF, platelet-derived growth factor (PDGF), angiopoietin 1 and 2 (Ang-1 and Ang-2), and TGF-β1 were quantified at different time points during vascular formation to clarify the role of the growth factors at a molecular level. The maturation and permeability of the microvessels were tested to validate the integrity of engineered vessels on the ECM scaffold. A multi-lineage differentiation assay of the prevascularized ECM scaffold was performed to examine the multi-potency preservation of hMSCs to determine whether their stem cell functions were retained throughout the pre-vascularization process.

2. Materials and Methods

2.1 Natural ECM scaffold preparation

The hDF-based ECM scaffolds were obtained as previously described (Xing et al., 2014). Briefly, the hDFs were cultured in Dulbecco's modified eagle medium (DMEM) with 20% fetal bovine serum (FBS) for 4 weeks with medium changes every 72 hours. The formed hDF sheets were then placed into the decellularization preparing buffer for 1 hour, which

contained 1 M NaCl, 10 mM Tris (Bio-rad, Hercules, CA), and 5 mM Ethylenediaminetetraacetic acid (EDTA, Sigma-Aldrich, St Louis, MO). The cell sheets were then transferred to the decellularization buffer with 0.5% sodium dodecyl sulfate (Bio-rad), 10 mM Tris, and 25 mM EDTA for 15 minutes at room temperature. After the decellularization process, the resulting ECM sheets were thoroughly washed with PBS, followed by incubation in DMEM and 1% penicillin/streptomycin for 48 h at room temperature before use.

2.2 Pre-vascularized ECM cultivation

The hMSCs were obtained from Texas A&M University Health Sciences Center. Passage 3 hMSCs at a density of 10,000 cells/cm^2 were seeded on the decellularized ECM sheets and cultured in complete culture medium (CCM, basal α-MEM, 20% FBS, 1% Pen/strep, and 1% L-glutamine) under either hypoxia (2% O_2) or normoxia (20% O_2) conditions for 7 days. Subsequently, the passage 3 HUVECs (Lonza, Walkersville, MD) were seeded at a density of 20,000 cells/cm^2 on top of the hMSCs/ECM sheets from both hypoxia and normoxia cultures. The co-cultures were maintained in normoxia (20% O_2) for up to 7 days in endothelial cell growth media (EGM, Lonza). The medium was changed every 48 hours.

2.3 Vasculature staining and imaging

The developing vasculature was examined by immunofluorescent staining. The co-cultures were washed with PBS, fixed and stained with mouse polyclonal antibody against human CD31 (Abcam, Cambridge, MA), and followed by DyLight 488 horse anti-mouse IgG secondary antibody (Vector laboratories, Burlingame, CA). The samples were washed and incubated in 4′, 6-diamidino-2-phenylindole (DAPI, Sigma-Aldrich) solution to stain the cell nuclei. Images were captured under an Olympus FV-1000 confocal microscopy. The vascular networks were quantified by ImageJ using previously described methods (Chen et al., 2009).

2.4 Proliferation assays

To investigate the proliferation of hMSCs in culture, Ki67, which labels active phases of the cell cycle G(1), S, G(2), and mitosis (Scholzen & Gerdes, 2000), and 5-Bromo-2′-Deoxyuridine (BrdU, Sigma-Aldrich) were selected. The BrdU assay was performed as previously described (Zhao et al., 2005). The samples were cultured in medium supplemented with BrdU (10 μM) for 24 hours. The percentage of BrdU positive cells was calculated as the number of BrdU positive cells normalized to the total number of cells obtained from DAPI staining.

2.5 Permeability and maturation assays

Texas Red-conjugated dextran (excitation/emission of 595/615 nm wavelength) with a molecular weight of 70 kDa (Invitrogen, Carlsbad, CA) was selected to visualize microvessel permeability, since this particle size is not able to leak across mature EC layers (Curry et al., 1983). All samples were incubated at 37 °C for 30 minutes with 5 mg/mL dextran in PBS. Excessive dextran was removed by washing in PBS (Grainger & Putnam, 2011). Washed samples were fixed with 4% PFA and counter stained with anti-CD31

(labeled with DyLight 488, green florescent). Alpha smooth muscle actin (α-SMA) and CD146 staining was performed with their primary antibodies (Abcam) and counter stained with CD31. Stained samples were imaged with confocal microscopy and z-stacked using ImageJ. Three samples from each group were imaged.

2.6 Enzyme-linked immunosorbent assay (ELISA) of soluble angiogenic growth factors

An ELISA assay was performed to quantify the growth factor presented in the cell culture medium. The cell culture medium was collected from the different groups at multiple time points. Ang-1, Ang-2, TGF-β1, VEGFA, and bFGF were quantified using ELISA kits (R&D Systems, Minneapolis, MN) following the manufacture's instruction. Optical density was measured with a plate reader (Molecular Devices, USA) at 450 nm with the correction wavelength set at 540 nm. A standard curve was made by GraphPad software. Experiments were triplicated, and each sample and standard was measured in duplicates.

2.7 Western blotting of angiogenic growth factors and cell surface receptors

Western blotting was performed to compare the relative amounts of growth factors VEGFA, bFGF, as well as cell surface receptor VEGFR2 in cultured prevascularized constructs. Radioimmunoprecipitation assay (RIPA) buffer with 1% protease inhibitors (Thermo Fisher) was used to collect cell lysates. Cell lysates were separated by sodium dodecyl sulfate–polyacrylamide gel electrophoresis (SDS-PAGE), and transferred onto a polyvinylidene fluoride (PVDF) membrane. The membranes were blocked with TBS supplied with 0.1% Tween-20 (TBST) (Thermo Fisher Scientific, Waltham, MA) and 5% dry milk (Bio-rad) and then incubated with primary antibodies overnight at 4 °C. A horseradish peroxidase–conjugated secondary antibody (1:3000, Bio-rad) was then added after washing, and incubated for 1 hour at room temperature. An ECL substrate (Bio-rad) was used to acquire the chemiluminescent signal, which was imaged using a FluorChem Imaging System (Alpha InnoTech, San Leandro, CA).

2.8 Real-time reverse transcription polymerase chain reaction (RT-qPCR)

RNA was extracted directly from the cultures using an RNeasy® extraction kit (Qiagen, Valencia, CA). Extracted RNA was reverse transcribed into cDNA using a reverse transcription kit (Life Technologies, Rockville, MD) and amplified by the StepOnePlus™ Real-Time PCR System (Applied Biosystems, Waltham, MA). SYBR® Green Real Time PCR Master Mixes (Life Technology) were used for quantification of fluorescent signal. Customized KiCqStart® SYBR® Green Primers (Sigma-Aldrich) were used, whose sequences are listed in Table 1. The GAPDH gene was used as an endogenous control. Data was analyzed using the $\Delta\Delta C_t$ method. Three individual samples were tested for statistical analysis.

2.9 Multi-lineage differentiation assays

To examine the multi-lineage differentiation ability of hMSCs after co-culture, osteogenic and adipogenic differentiation assays were performed (Grayson et al., 2007). For osteogenesis, vascularized co-cultures were replaced with osteogenic induction medium (CCM supplemented with 100 nM dexamethasone, 10 mM sodium-β-glycerophosphate, and

0.05 mM ascorbic acid-2-phosphate, Sigma-Aldrich). After 2 weeks, the alkaline phosphatase (ALP) activity of the cultures was evaluated following our published method (Xing, Qian, et al., 2015). The mineralization of the cultures was visualized by Von Kossa staining (Grayson et al., 2004). The calcium concentration was determined by ion coupled plasma (ICP) spectroscopy (Leeman Laboratories, Lowell, MA). To do this, the specimens were isolated from cell culture and dissolved in 12 M HCL and diluted 1:10 for the ICP measurements. For adipogenic differentiation, vascularized co-cultures were placed in adipogenic induction medium (CCM supplemented with 0.2 mM indomethacin, 0.5 mM isobutyl-1-methylxanthine, 1 mM dexamethasone, and 10 mg/mL insulin, Sigma-Aldrich) for 21 days. Adipogenic differentiation was quantified by Oil Red O staining of the lipid vacuoles as previously described (Kim & Ma, 2013). Images were taken using an Olympus BX51 microscope. After imaging, the dye retained by the cells was eluted by isopropanol and the absorbance was measured at a wavelength of 540 nm and normalized to cell number. Three independent samples were tested under each experimental condition. Undifferentiated samples cultured under the same condition in EGM were used as control.

2.10 Statistical analysis

The results were reported as mean ± standard deviation. Post hoc analysis was conducted using Tukey's procedure. Results were considered statistically significant for $p < 0.05$.

3. Results

3.1 Microvessel formation

Immunofluorescent staining of CD31, as shown in Figure 1a, revealed a striking increase in microvessel density for H-groups at days 3, 5, and 7. At days 5 and 7, more branches were observed in H-groups than N-groups. Quantification of the total vessel length (Figure 1b) showed that H-groups had a significantly longer total vessel length than N-groups throughout the entire 7-day culture period ($p < 0.01$). The average vessel length of H-groups was also significantly higher than N-groups ($p < 0.05$, day 3 & day 5; $p < 0.01$, day 7) (Figure 1c). The average number of branches per vessel network in H-groups was significantly higher than N-groups at day 5 and day 7 ($p < 0.01$) (Figure 1d). No significant difference was found at day 3, which was expected due to both cultures still undergoing vessel formation. The average vessel surface area fraction is an indicator of the microvessel density, which was significantly higher in H-groups (day 7: 25.35 ± 1.62, % of area) than their normoxia counterparts (day 7: 18.33 ± 1.49, % of area, $p < 0.01$) (Figure 1e). Measurements of lumens per square millimeter showed that H-groups had significantly more lumens formed than N-groups ($p < 0.01$ for day 3, $p < 0.05$ for day 5 and day 7) (Figure 1f). The vessel diameter was 33% narrower in the H-groups ($p < 0.01$) (Figure 1g).

3.2 Cell proliferation in prevascularized samples

As shown in Figure 2a and 2b, 13% more Ki67 positive cells were present in the H-group than the N-group at day 7 ($p < 0.01$). The BrdU staining, as shown in green on Figure 2c, also showed more proliferative cells in the vascular network of the H-group, while fewer proliferating cells were detected in the N-group. The BrdU quantitative analysis demonstrated 20% more proliferating cells in H-groups than N-groups (Figure 2d, $p < 0.01$).

3.3 Permeability and maturation of microvessels

A dextran assay was performed to test the permeability of the microvessels formed in different culture conditions. From Figure 3a, dextran particles were built up around the microvessels in the H-group at day 7. However, no clear boundaries were recognized in the N-group, and some dextran particles were found inside the vessel. α-SMA-expressing pericytes (red color on Figure 3b) were observed surrounding the microvessels and clear lumens were visualized in the cross-sectional view of H-groups at day 7. In the N-groups, α-SMA-expressing cells were detected in the scaffold, but none of them were coupled around the vessels. The cross-sectional view of N-group samples also proved that α-SMA-expressing cells were not supporting the microvessel lumen. CD146 positive staining was found surrounded by the microvessels (CD31 positive staining) in both H- and N-groups, while the H-groups showed larger and clearer margins in CD146 stained area than N-groups (Figure 3c). Western blot results evidenced that the CD146 expression was 2.75 folds higher in H-groups than N-groups ($p < 0.05$) (Figure 3d, 3e).

3.4 Angiogenic growth factor secretion in growth medium

The concentrations of angiogenic growth factors VEGF, bFGF, TGF-β1, Ang-1, and Ang-2 in culture medium supernatant of the samples were quantified by ELISA (Figure 4). In our previous study, we have found the concentration of VEGF in the culture medium was approximately 3,000 pg/mL, the bFGF concentration was 10,000 pg/mL, TGF-β1 was 200 pg/mL, and no trace of Ang-1 and Ang-2 were detected (Zhang et al., 2016). The medium concentrations of VEGF and bFGF in the ECM/hMSCs/ECs dramatically decreased during the entire 7-day co-culture period, although they were significantly higher in H-groups than N-groups ($p < 0.01$) (Supplemental Figure 1). The day 7 results also showed that they were drastically low in all samples (Figure 4a, 4b). The co-culture with ECs further decreased the VEGF concentration in both hMSCs and ECM/hMSCs samples (Figure 4a), while the bFGF concentration increased. In addition, the bFGF concentration in ECM/hMSCs/ECs samples was significantly higher than hMSCs/ECs ($p < 0.01$) (Figure 4b). The TGF-β1 was significantly decreased by hypoxia culture of hMSCs in hMSCs/ECs and ECM/hMSCs/ECs samples ($p < 0.05$) (Figure 4c). Higher Ang-1 concentration in the medium was detected in H-groups when ECM was present, while the opposite phenomenon was observed when ECM was absent (Figure 4d). The medium concentration of Ang-2 increased 100 folds in hMSCs/ECs and ECM/hMSCs/ECs than the groups without ECs ($p < 0.01$) (Figure 4e). However, hypoxia does not have significant effects on Ang-2 secretion.

3.5 Protein and gene expression of angiogenic growth factors in vascularized ECM constructs

Western blotting and RT-qPCR were conducted to examine the transcriptional and translational expression of angiogenic growth factors in vascularized ECM constructs at day 7 (Figure 5). No significant difference was observed in VEGFA expression at the protein level (Figure 5a). However, mRNA expression of VEGFA in the H-group of ECM/hMSCs/ECs was 300 fold higher than all the other groups (Figure 5d). The bFGF protein expression was lowered by hypoxia when ECM was present (Figure 5b), and the H-group of ECM/hMSCs/ECs has the lowest expression. Nevertheless, the mRNA expression of bFGF

in co-cultured H-groups was 50 fold higher than N-groups (Figure 5e). VEGFR2, the main receptor for VEGFA, showed higher expression at protein level in the H-groups (Figure 5c). However, at gene level, it was 25 fold more expressed in the normoxia samples than the hypoxia samples (Figure 5f). To further examine how the cells responded to hypoxia on the molecular level, mRNA expressions of HIF-1α (upstream regulator of VEGFA) and PDGFB were investigated. Results suggested that in hypoxia ECM/hMSCs/ECs samples, the expression of HIF-1α was increased by 15 fold compared to the N-groups (Figure 5g), which led to the drastic increase of VEGFA mRNA expression. However, the mRNA expression of PDGFB was not influenced by the hypoxia culture of hMSCs (Figure 5h).

3.6 Multi-lineage differentiation of hMSCs post vascularization

Osteogenic and adipogenic differentiation assays were performed to determine whether hMSCs still maintained their multi-potency after co-culturing with ECs. The Von Kossa staining showed that after the osteogenic differentiation of ECM/hMSCs/ECs constructs for 14 days, the microvessels still retained their structure in both hypoxia and normoxia samples (Figure 6a). In addition, more calcium was deposited in the hypoxia samples than their normoxia counterparts, which was further confirmed by the quantitative calcium analysis ($p < 0.05$) (Figure 6b). The ALP characterization also showed higher ALP activity in the H-groups ($p < 0.01$) (Figure 6c). The qPCR analysis demonstrated higher expression of osteonectin in H-group, as seen in Figure 6d ($p < 0.01$). Correspondingly, the expression of stemness genes, Oct-4 and Rex-1, were scarcely detected due to the complete osteogenic differentiation of hMSCs. After 21 days adipogenic differentiation of the ECM/hMSCs/ECs constructs, the Oil red O staining (Figure 6e) and quantification (Figure 6f) showed that the hypoxia culture significantly enhanced the adipogenic differentiation of hMSCs ($p < 0.05$). The qPCR analysis also demonstrated a higher expression of adipose differentiation indicators PPARG (5.2 folds) and CEBPA (1.6 folds) (Figure 6g). The expression of stemness genes Oct-4 and Rex-1 was drastically lowered due to the adipogenic differentiation of hMSCs.

4. Discussion

A major obstacle of tissue engineering is to sustain the growth and metabolism of engineered tissues with consistent oxygen and nutrient supplies (Zhang et al., 2016). Cell-based pre-vascularized tissues will not only receive the benefit of enhanced tissue regeneration, but also potentially serve as bench top study models for cancer progression and drug screening. Conventional co-culture prevascularization strategies, utilizing fibroblasts and SMCs, are capable of stabilizing and supporting vasculatures formed by ECs, but the cells employed to develop the constructs lack potential to promote regeneration at injury sites.

We have previously demonstrated the feasibility of creating a prevascularized hMSC cell sheet via co-culture of hMSCs with ECs (Zhang et al., 2016). However, the hMSC cell sheet was mechanically weak and the multi-potency of the hMSCs was partially sacrificed due to the long-term culture (4 weeks). To overcome these problems, a purely natural nanofibrous ECM scaffold that we previously created, which contains elastin and has relatively high

mechanical strength, was selected as a replacement for the ECM secreted by hMSCs (Xing et al., 2017; Xing, Yates, et al., 2015). Moreover, our previous study has demonstrated better vascular network formation by growing hMSC cell sheets under physiologically low oxygen (2% O_2) prior to co-culture with ECs (Zhao et al., 2010). The 2% O_2 culture of hMSCs maintained the stemness and enhanced the overall quality of the engineered microvessels. In this study, similar combinations of culture conditions were used to stimulate microvessel formation on the ECM scaffolds while reducing culture time from 6 weeks (4 week culture of hMSCs under hypoxia following by 2 weeks co-culture with ECs) to 2 weeks (1 week culture of hMSCs under hypoxia following by 1 week co-culture with ECs). It was expected that a prevascularized hMSC/ECM sheet with mature microvessels and well maintained hMSC stemness would be created.

Compared with other materials for cell-based prevascularization strategies, the fibroblast-derived ECM scaffold has superior characteristics in multiple aspects such as better surface properties for cell adhesion, stronger mechanical properties, and shorter culture time (Jinling et al., 2014; Lin et al., 2012; Ren et al., 2014; Zhang et al., 2016). hMSCs were grown on the ECM scaffold for 7 days under both hypoxia and normoxia conditions (Figure 1). It was found that ECM supported microvessel formation in both conditions within 7 days after the EC seeding, with the H-groups showing significantly higher microvessel density than N-groups. The average microvessel length formed on the ECM scaffold (2 mm) was longer than those grown on hMSCs cell sheet (1.5 mm) as previously reported (Zhang et al., 2016). The microvessels formed on the ECM scaffold were also obviously denser than a similar hMSC sheet/ECs co-culture that was grown on glass coverslips (Zhang et al., 2016), suggesting the beneficial effects of ECM in vascularization. Compared with other *in vitro* studies of vascularization on different constructs (Chen et al., 2012; Ren et al., 2014; Yang et al., 2013), the vasculature formed on the ECM scaffold was more robust and denser. It has also been confirmed that ECM protein fibrils, when in a physiological density, resulted in robust neovascular formation both *in vitro* and *in vivo* (Kniazeva et al., 2010). This finding is also consistent with our results, which showed the supporting role of natural ECM fibers in angiogenesis.

The hMSCs can specifically play the role of pericytes, which express adhesion molecules, respond to angiogenic stimuli, and stabilize vasculatures (Au et al., 2008; da Silva Meirelles et al., 2015; Wong et al., 2015). hMSCs also rescue the phenotypical change of ECs during angiogenesis, thereby preventing the degradation of the growing vessels (Kniazeva et al., 2010). Using hypoxia cultivation, this supporting function of hMSCs can be further reinforced. In this study, the number of cells that were under active cell cycle was significantly increased by hypoxia cultivation (Figure 2a and 2b). The integration of microvessels formed on ECM scaffolds showed strong dependence on the number of proliferating cells. Quantitative analysis supported the observation that more proliferative cells were present in H-groups (Figure 2c & 2d). A study on the maturation and permeability of the neovasculature has shown that hMSCs play vital roles to enhance stabilization and decrease the permeability of the vasculature (Grainger & Putnam, 2011). Another study demonstrated that only CD146-expressing hMSCs could function as pericytes to stabilize microvessels (Blocki et al., 2013). Findings from these studies are consistent with our dextran permeability assay results, which showed that the maturation of the vasculature was

enhanced by hMSCs grown from hypoxic condition (Figure 3a). Moreover, more α-SMA and CD146 positive hMSCs were present around vasculatures in H-groups, surrounding more complete lumen structure with smoother vessel margin (Figure 1g, 3b & 3c). The protein expression level of CD146 was also up-regulated in the H-group, suggesting more hMSCs were providing a pericyte function (Figure 3d & 3e). In contrast, fewer α-SMA and CD 146 positive hMSCs could be detected in N-groups, which resulted in larger and flatter lumen structures as well as loosely arranged vasculatures with impaired insulation. These results proved that hMSCs from hypoxia cultivation were crucial for constructing mature microvascular structures.

It has been proven that angiogenic growth factor incorporation in scaffolds can promote angiogenesis *in vitro* (Zisch et al., 2003). Thus vascular formation could be attributed to growth factors that accumulated in the ECM scaffold (Xing et al., 2014). Vascular growth factors such as VEGF, bFGF, and PDGF can significantly promote angiogenesis (Armulik et al., 2005). To investigate the mechanism of vascular formation on ECM scaffolds, angiogenic growth factors were examined during the vascular progression. The results of ECM/hMSCs/ECs samples showed that the concentrations of VEGF and bFGF during the 7 day co-culture were drastically lower than their initial concentrations supplied by the fresh medium (Supplemental Figure 1), suggesting the two growth factors were rapidly consumed by the cells, similar to the finding of another group (Griffith & George, 2009). Moreover, at day 7 the co-cultures consumed more VEGF but less bFGF than the hMSC only group due to the vasculature formation and maturation (Figures 4a & 4b). Overall, the hypoxia groups exhibited higher concentrations of the two growth factors in all the groups. It is possible that hypoxia culture maintained healthier hMSCs, which increased the secretion of VEGF and bFGF (Schinköthe et al., 2008). The cultures significantly increased the concentrations of TGF-β1, Ang-1, and Ang-2 in the medium at day 7 (Figures 4c, 4d & 4e). The TGF-β1 was up-regulated (Figure 4c) in N-groups, possibly because of the needs of pericytes recruitment for vessel stabilization, as anticipated by the literature (Akhurst et al., 1990). This up-regulation of TGF-β1 also complemented the observation that fewer mural cells in N-groups, as suggested by CD 146 staining (Figure 3c). The Ang-1 secretion was up-regulated by the presence of ECM in H-groups, indicating the active angiogenesis activity in a more biomimetic environment. When ECM was absent, higher Ang-1 was secreted by N-groups for neovasculature maturation and stabilization. The co-cultures also increased the Ang-2 secretion, because only ECs released Ang-2 to stimulate sprouting and branching during the angiogenesis (Zhao et al., 2015). The Ang-2 secretion was down regulated at day 7 by the presence of ECM, suggesting the more matured and stabilized vascular networks were formed in a more biomimetic environment (Hakanpaa et al., 2015).

The hypoxia condition of hMSCs enhanced the mRNA expression of VEGFA and bFGF. VEGF receptor 2 (VEGFR2) was exclusively expressed by ECs when proliferation and migration of the ECs were elevated for neovascular formation (Holmes et al., 2007). This study showed that protein expression of VEGFR2 significantly increased (Figure 5c), while mRNA expression of VEGFR2 drastically decreased in H-groups (Figure 5f). It is possible that ECs in H-groups highly produced VEGFR2, which suppressed the sprouting of neovasculature yet stimulated the maturation of existing vasculature. In contrast, N-groups exhibited higher mRNA expression of VEGFR2, which was crucial for continuing the

neovascular formation (Huang et al., 2016). The decreased mRNA expression of PDGFB (Figure 5h) strongly supported this interpretation, because during rapid angiogenic sprouting, PDGFB is intensively secreted by ECs to recruit pericytes for stabilizing neovasculatures (Chang et al., 2013). On the other hand, due to the delayed timeline of neovascular formation in N-groups, the mRNA production of both VEGFR2 and PDGF was increased because of the urgent needs of recruiting pericytes to stabilize the rapidly sprouting vasculatures (Armulik et al., 2005). The pattern of angiogenic growth factors and receptor expression explained the better microvessel morphology observed in the H-groups during the co-culture stage (Figure 1b). Other than VEGF and bFGF, hypoxia stabilized intracellular level of HIF-1α in hMSCs regulates the continuous vessel remodeling by controlling the VEGF and bFGF secretion (Lin et al., 2008). In our study, transcriptional upregulation of HIF-1α was observed in H-group during co-culture, which corresponded to the mRNA elevation of both VEGF and bFGF (Pugh & Ratcliffe, 2003; Tamama et al., 2011). All of these factors contributed to the formation of a robust and mature vascular network on the ECM scaffold.

It was crucial for the bulk hMSCs to maintain their undifferentiated status for functional engineered tissue construction (Parekkadan & Milwid, 2010). Previous research has shown that the multi-potency of hMSCs gradually decreased over long-term culture (Xing, Qian, et al., 2015). By shortening the overall cultivation time and utilizing physiologically low oxygen culture conditions, the differentiation capability of hMSCs was well preserved. Osteogenic and adipogenic differentiation assays proved that H-groups had better differentiation capability than their N-group counterparts (Figure 6). Previous studies showed that osteogenic differentiation of hMSCs was favorable on the ECM scaffold, and could be enhanced by ECs (Pirraco et al., 2014; Xing, Qian, et al., 2015), suggesting that prevascularized ECM scaffolds could potentially serve as a building material for engineering prevascularized bone tissues. Higher ALP activity and calcium deposition were detected in the H-groups than N-groups after 14 days osteogenic induction, suggesting hMSCs in H-groups maintained higher stemness. We have also observed that the adipogenic differentiation potential was not sacrificed in the prevascularized ECM, which enables the multifunctional applications of the prevascularized ECM. Overall, hMSCs in H-groups effectively maintained their multipotency. Therefore, the prevascularized ECM can be potentially utilized in various tissue engineering applications.

5. Conclusions

In this study, we had created a prevascularized hMSC/ECM sheet by firstly growing hMSCs on an ECM scaffold and then co-culturing ECs on top of the hMSC sheet. Physiologically low oxygen (2% O_2, hypoxia) was introduced during hMSCs culture to maintain their stemness while enhancing their secretion of angiogenic factors. The hMSCs functioned as pericytes to stabilize and support the microvessels. Results showed that branched and matured vasculature networks were formed on the ECM scaffolds, while the hypoxic culture of hMSCs further preserved the multi-potency of the hMSCs and improved the microvasculature structure. The prevascularized hMSC/ECM sheet holds great potential for engineering multiple completely biological and prevascularized tissues.

Supplementary Material

Refer to Web version on PubMed Central for supplementary material.

Acknowledgments

This study was supported by the National Institutes of Health (1R15HL115521-01A1 and R15CA202656), the National Science Foundation (1703570), and Research Excellence Funds from both the Portage Health Foundation (PHF) and Michigan Technological University to F.Z. It was also supported by the National Natural Science Foundation of China (NSFC: 81471883) to S.Q.

References

Aguirre A, Planell JA, Engel E. Dynamics of bone marrow-derived endothelial progenitor cell/mesenchymal stem cell interaction in co-culture and its implications in angiogenesis. Biochem Biophys Res Commun. 2010; 400(2):284–291. [PubMed: 20732306]

Akhurst RJ, Lehnert SA, Faissner A, Duffie E. TGF beta in murine morphogenetic processes: the early embryo and cardiogenesis. Development. 1990; 108(4):645–656. [PubMed: 1696875]

Armulik A, Abramsson A, Betsholtz C. Endothelial/pericyte interactions. Circ Res. 2005; 97(6):512–523. [PubMed: 16166562]

Au P, Tam J, Fukumura D, Jain RK. Bone marrow–derived mesenchymal stem cells facilitate engineering of long-lasting functional vasculature. Blood. 2008; 111(9):4551–4558. [PubMed: 18256324]

Barati D, Shariati SRP, Moeinzadeh S, Melero-Martin JM, Khademhosseini A, Jabbari E. Spatiotemporal release of BMP-2 and VEGF enhances osteogenic and vasculogenic differentiation of human mesenchymal stem cells and endothelial colony-forming cells co-encapsulated in a patterned hydrogel. J Controlled Release. 2016; 223:126–136.

Blocki A, Wang Y, Koch M, Peh P, Beyer S, Law P, … Raghunath M. Not All MSCs Can Act as Pericytes: Functional In Vitro Assays to Distinguish Pericytes from Other Mesenchymal Stem Cells in Angiogenesis. Stem Cells Dev. 2013; 22(17):2347–2355. [PubMed: 23600480]

Chang WG, Andrejecsk JW, Kluger MS, Saltzman WM, Pober JS. Pericytes modulate endothelial sprouting. Cardiovasc Res. 2013; 100(3):492–500. [PubMed: 24042014]

Chen X, Aledia A, Ghajar C, Griffith C, Putnam A, Hughes CCW, George S. Prevascularization of a fibrin-based tissue construct accelerates the formation of functional anastomosis with host vasculature. Tissue Eng, Part A. 2009; 15(6):1363–1371. [PubMed: 18976155]

Chen YC, Lin RZ, Qi H, Yang Y, Bae H, Melero-Martin JM, Khademhosseini A. Functional Human Vascular Network Generated in Photocrosslinkable Gelatin Methacrylate Hydrogels. Adv Funct Mater. 2012; 22(10):2027–2039. [PubMed: 22907987]

Costa, M., Pirraco, RP., Cerqueira, MT., Reis, RL., Marques, AP. Growth Factor-Free Pre-vascularization of Cell Sheets for Tissue Engineering. In: Turksen, K., editor. Stem Cell Heterogeneity: Methods and Protocols. New York, NY: Springer New York; 2016. p. 219-226.

Curry FE, Huxley VH, Adamson RH. Permeability of single capillaries to intermediate-sized colored solutes. Am J Physiol. 1983; 245(3):H495–505. [PubMed: 6604463]

Czajka CA, Drake CJ. Self-assembly of prevascular tissues from endothelial and fibroblast cells under scaffold-free, nonadherent conditions. Tissue Eng, Part A. 2015; 21(1–2):277–287. [PubMed: 25076018]

da Silva Meirelles L, Malta TM, de Deus Wagatsuma VM, Palma PVB, Araújo AG, Ribeiro Malmegrim KC, … Covas DT. Cultured Human Adipose Tissue Pericytes and Mesenchymal Stromal Cells Display a Very Similar Gene Expression Profile. Stem Cells Dev. 2015; 24(23):2822–2840. [PubMed: 26192741]

Grainger S, Putnam A. Assessing the permeability of engineered capillary networks in a 3D culture. PLoS ONE. 2011; 6(7):e22086. [PubMed: 21760956]

Grayson W, Ma T, Bunnell B. Human mesenchymal stem cells tissue development in 3D PET matrices. Biotechnol Progr. 2004; 20(3):905–912.

Grayson W, Zhao F, Bunnell B, Ma T. Hypoxia enhances proliferation and tissue formation of human mesenchymal stem cells. Biochem Biophys Res Commun. 2007; 358(3):948–953. [PubMed: 17521616]

Griffith CK, George SC. The Effect of Hypoxia on In Vitro Prevascularization of a Thick Soft Tissue. Tissue Eng, Part A. 2009; 15(9):2423–2434. [PubMed: 19292659]

Guerreiro SG, Oliveira MJ, Barbosa MA, Soares R, Granja PL. Neonatal human dermal fibroblasts immobilized in RGD-alginate induce angiogenesis. Cell Transplant. 2014; 23(8):945–957. [PubMed: 23866308]

Hakanpaa L, Sipila T, Leppanen VM, Gautam P, Nurmi H, Jacquemet G, … Saharinen P. Endothelial destabilization by angiopoietin-2 via integrin β1 activation. Nature Communications. 2015; 6:5962.

Holmes K, Roberts OL, Thomas AM, Cross MJ. Vascular endothelial growth factor receptor-2: Structure, function, intracellular signalling and therapeutic inhibition. Cell Signalling. 2007; 19(10):2003–2012. [PubMed: 17658244]

Huang M, Qiu Q, Xiao Y, Zeng S, Zhan M, Shi M, … Xu H. BET Bromodomain Suppression Inhibits VEGF-induced Angiogenesis and Vascular Permeability by Blocking VEGFR2-mediated Activation of PAK1 and eNOS. Sci Rep. 2016; 6:23770. [PubMed: 27044328]

Jinling M, Fang Y, Sanne KB, Henk-Jan P, Marco NH, Juli P, … Jeroen JJPvdB. In vitro and in vivo angiogenic capacity of BM-MSCs/HUVECs and AT-MSCs/HUVECs cocultures. Biofabrication. 2014; 6(1):015005. [PubMed: 24429700]

Kim J, Ma T. Autocrine fibroblast growth factor 2-mediated interactions between human mesenchymal stem cells and the extracellular matrix under varying oxygen tension. J Cell Biochem. 2013; 114(3):716–727. [PubMed: 23060043]

Kniazeva E, Kachgal S, Putnam AJ. Effects of Extracellular Matrix Density and Mesenchymal Stem Cells on Neovascularization In Vivo. Tissue Eng, Part A. 2010; 17(7–8):905–914. [PubMed: 20979533]

Lin JL, Wang MJ, Lee D, Liang CC, Lin S. Hypoxia-inducible factor-1alpha regulates matrix metalloproteinase-1 activity in human bone marrow-derived mesenchymal stem cells. FEBS Lett. 2008; 582(17):2615–2619. [PubMed: 18588890]

Lin RZ, Moreno-Luna R, Zhou B, Pu WT, Melero-Martin JM. Equal modulation of endothelial cell function by four distinct tissue-specific mesenchymal stem cells. Angiogenesis. 2012; 15(3):443–455. [PubMed: 22527199]

Lovett M, Lee K, Edwards A, Kaplan DL. Vascularization Strategies for Tissue Engineering. Tissue Eng, Part B. 2009; 15(3):353–370.

Mercado-Pagán ÁE, Stahl AM, Shanjani Y, Yang Y. Vascularization in Bone Tissue Engineering Constructs. Ann Biomed Eng. 2015; 43(3):718–729. [PubMed: 25616591]

Parekkadan B, Milwid JM. Mesenchymal Stem Cells as Therapeutics. Annu Rev Biomed Eng. 2010; 12:87–117. [PubMed: 20415588]

Pirraco RP, Iwata T, Yoshida T, Marques AP, Yamato M, Reis RL, Okano T. Endothelial cells enhance the in vivo bone-forming ability of osteogenic cell sheets. Lab Invest. 2014; 94(6):663–673. [PubMed: 24709778]

Pugh CW, Ratcliffe PJ. Regulation of angiogenesis by hypoxia: role of the HIF system. Nat Med. 2003; 9(6):677–684. [PubMed: 12778166]

Radisic M, Park H, Chen F, Salazar-Lazzaro JE, Wang Y, Dennis R, … Vunjak-Novakovic G. Biomimetic approach to cardiac tissue engineering: oxygen carriers and channeled scaffolds. Tissue Eng. 2006; 12(8):2077–2091. [PubMed: 16968150]

Ren L, Ma D, Liu B, Li J, Chen J, Yang D, Gao P. Preparation of three-dimensional vascularized MSC cell sheet constructs for tissue regeneration. BioMed Res Int. 2014; 2014:301279. [PubMed: 25110670]

Sakaguchi K, Shimizu T, Okano T. Construction of three-dimensional vascularized cardiac tissue with cell sheet engineering. J Controlled Release. 2015; 205:83–88.

Sakamoto N, Kiuchi T, Sato M. Development of an endothelial-smooth muscle cell coculture model using phenotype-controlled smooth muscle cells. Ann Biomed Eng. 2011; 39(11):2750–2758. [PubMed: 21811870]

Schinköthe T, Bloch W, Schmidt A. In Vitro Secreting Profile of Human Mesenchymal Stem Cells. Stem Cells Dev. 2008; 17(1):199–206. [PubMed: 18208373]

Scholzen T, Gerdes J. The Ki-67 protein: from the known and the unknown. J Cell Physiol. 2000; 182(3):311–322. [PubMed: 10653597]

Shamis Y, Silva EA, Hewitt KJ, Brudno Y, Levenberg S, Mooney DJ, Garlick JA. Fibroblasts Derived from Human Pluripotent Stem Cells Activate Angiogenic Responses In Vitro and In Vivo. PLoS ONE. 2013; 8(12):e83755. [PubMed: 24386271]

Sorrell JM, Baber MA, Caplan AI. Human dermal fibroblast subpopulations; differential interactions with vascular endothelial cells in coculture: Nonsoluble factors in the extracellular matrix influence interactions. Wound Repair and Regeneration. 2008; 16(2):300–309. [PubMed: 18318814]

Tamama K, Kawasaki H, Kerpedjieva SS, Guan J, Ganju RK, Sen CK. Differential roles of hypoxia inducible factor subunits in multipotential stromal cells under hypoxic condition. J Cell Biochem. 2011; 112(3):804–817. [PubMed: 21328454]

Tunyogi-Csapo M, Koreny T, Vermes C, Galante JO, Jacobs JJ, Glant TT. Role of fibroblasts and fibroblast-derived growth factors in periprosthetic angiogenesis. Journal of Orthopaedic Research. 2007; 25(10):1378–1388. [PubMed: 17557346]

Wenger A, Stahl A, Weber H, Finkenzeller G, Augustin HG, Stark GB, Kneser U. Modulation of in vitro angiogenesis in a three-dimensional spheroidal coculture model for bone tissue engineering. Tissue Eng. 2004; 10(9–10):1536–1547. [PubMed: 15588413]

Wong SP, Rowley JE, Redpath AN, Tilman JD, Fellous TG, Johnson JR. Pericytes, mesenchymal stem cells and their contributions to tissue repair. Pharmacol Ther. 2015; 151:107–120. [PubMed: 25827580]

Xing Q, Qian Z, Kannan B, Tahtinen M, Zhao F. Osteogenic Differentiation Evaluation of an Engineered Extracellular Matrix Based Tissue Sheet for Potential Periosteum Replacement. ACS Appl Mater Interfaces. 2015; 7(41):23239–23247. [PubMed: 26419888]

Xing Q, Qian Z, Tahtinen M, Yap AH, Yates K, Zhao F. Aligned Nanofibrous Cell-Derived Extracellular Matrix for Anisotropic Vascular Graft Construction. Adv Healthcare Mater. 2017 1601333-n/a.

Xing Q, Vogt C, Leong K, Zhao F. Highly Aligned Nanofibrous Scaffold Derived from Decellularized Human Fibroblasts. Adv Funct Mater. 2014; 24(20):3027–3035. [PubMed: 25484849]

Xing Q, Yates K, Tahtinen M, Shearier E, Qian Z, Zhao F. Decellularization of Fibroblast Cell Sheets for Natural Extracellular Matrix Scaffold Preparation. Tissue Engineering Part C, Methods. 2015; 21(1):77–87. [PubMed: 24866751]

Yang P, Huang X, Shen J, Wang CS, Dang XQ, Mankin H, … Wang KZ. Development of a new pre-vascularized tissue-engineered construct using pre-differentiated rADSCs, arteriovenous vascular bundle and porous nano-hydroxyapatide-polyamide 66 scaffold. Bmc Musculoskeletal Disorders. 2013:14. [PubMed: 23297850]

Zhang L, Xing Q, Qian Z, Tahtinen M, Zhang Z, Shearier E, … Zhao F. Hypoxia Created Human Mesenchymal Stem Cell Sheet for Prevascularized 3D Tissue Construction. Adv Healthcare Mater. 2016; 5(3):342–352.

Zhao F, Pathi P, Grayson W, Xing Q, Locke B, Ma T. Effects of oxygen transport on 3-d human mesenchymal stem cell metabolic activity in perfusion and static cultures: experiments and mathematical model. Biotechnol Progr. 2005; 21(4):1269–1280.

Zhao F, Veldhuis JJ, Duan Y, Yang Y, Christoforou N, Ma T, Leong KW. Low Oxygen Tension and Synthetic Nanogratings Improve the Uniformity and Stemness of Human Mesenchymal Stem Cell Layer. Molecular Therapy. 2010; 18(5):1010–1018. [PubMed: 20179678]

Zhao Q, Hu J, Xiang J, Gu Y, Jin P, Hua F, … Ye X. Intranasal administration of human umbilical cord mesenchymal stem cells-conditioned medium enhances vascular remodeling after stroke. Brain Res. 2015; 1624:489–496. [PubMed: 26279113]

Zisch AH, Lutolf MP, Ehrbar M, Raeber GP, Rizzi SC, Davies N, … Hubbell JA. Cell-demanded release of VEGF from synthetic, biointeractive cell-ingrowth matrices for vascularized tissue growth. FASEB J. 2003

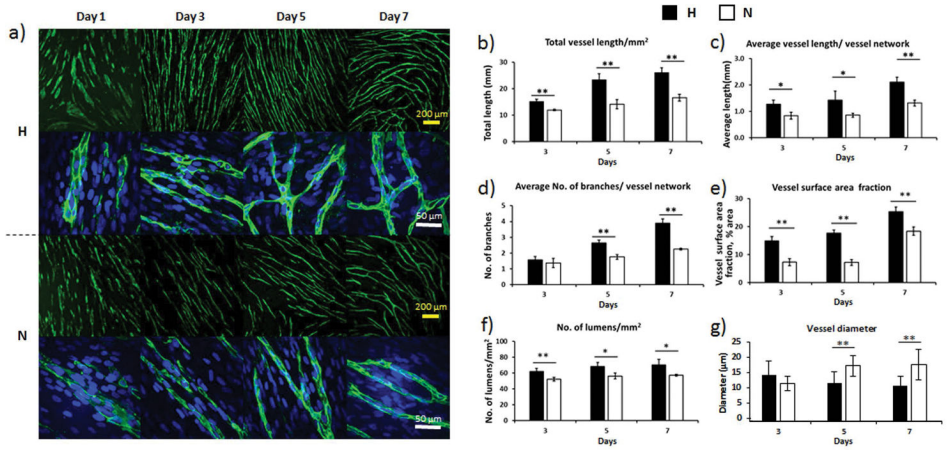

Figure 1.

Vasculature formation on ECM scaffolds. a) Low and high magnification images of microvessels at different time points. The hypoxia groups (H-groups) had higher density and more branches than the normoxia groups (N-groups) at day 5 and day 7. The microvessels were stained with CD31 primary antibody (green). The cell nuclei were stained with DAPI (blue). Quantification of microvessel total (b) and average (c) length, branches (d), surface area fraction (e), lumens (f), and average diameter (g) for both H-groups and N-groups. Hypoxia enhanced the vessel structures in all categories. (*$p < 0.05$, **$p < 0.01$)

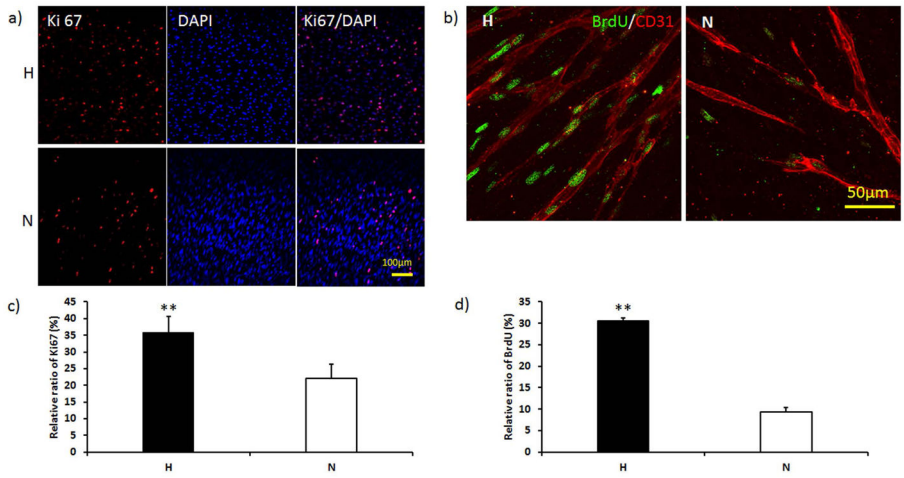

Figure 2.

Cell proliferation in both H-groups and N-groups at day 7. a) Ki 67 (red) staining showed that more active cells were present after hypoxia culture. b) BrdU (green) positive staining showed more proliferative cells surrounding the microvessels in the H-group. Vessels were labeled with CD31 (red). c) Quantification of Ki 67 showed that the active cell ratio was significantly higher in the H-group than the N-group. d) Quantification of BrdU showed that the proliferating cell ratio was significantly higher in the H-group. (**$p < 0.01$)

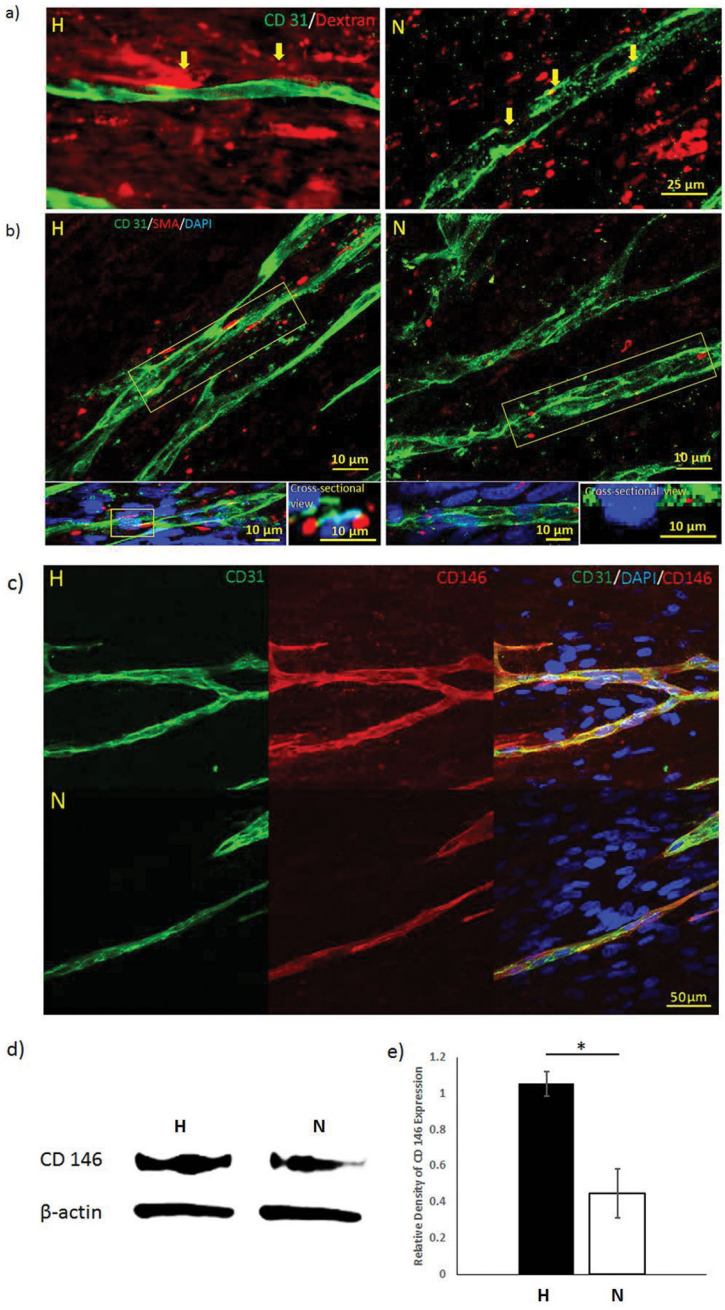

Figure 3.

(a) Dextran permeability assay of hypoxia and normoxia samples at day 7. Accumulated dextran dye was observed surrounding the boundary of the microvessels in hypoxia samples, as pointed by the yellow arrows. In comparison, dextran particles were found inside the microvessels in normoxia samples. (b) Confocal images of α-SMA-expressing hMSCs around the vasculatures. The side view of the vasculature showed α-SMA-expressing hMSCs supported the microvessel lumen in the H-groups, but not in the N-groups. Immunofluorescent staining of CD146 pericyte marker for H-group and N-group (c) demonstrated that both groups have positively stained vessel structure. CD146 expression

(d) was performed by western blot and quantified (e) to show that more CD146 was expressed in the H-group. (*$p < 0.05$)

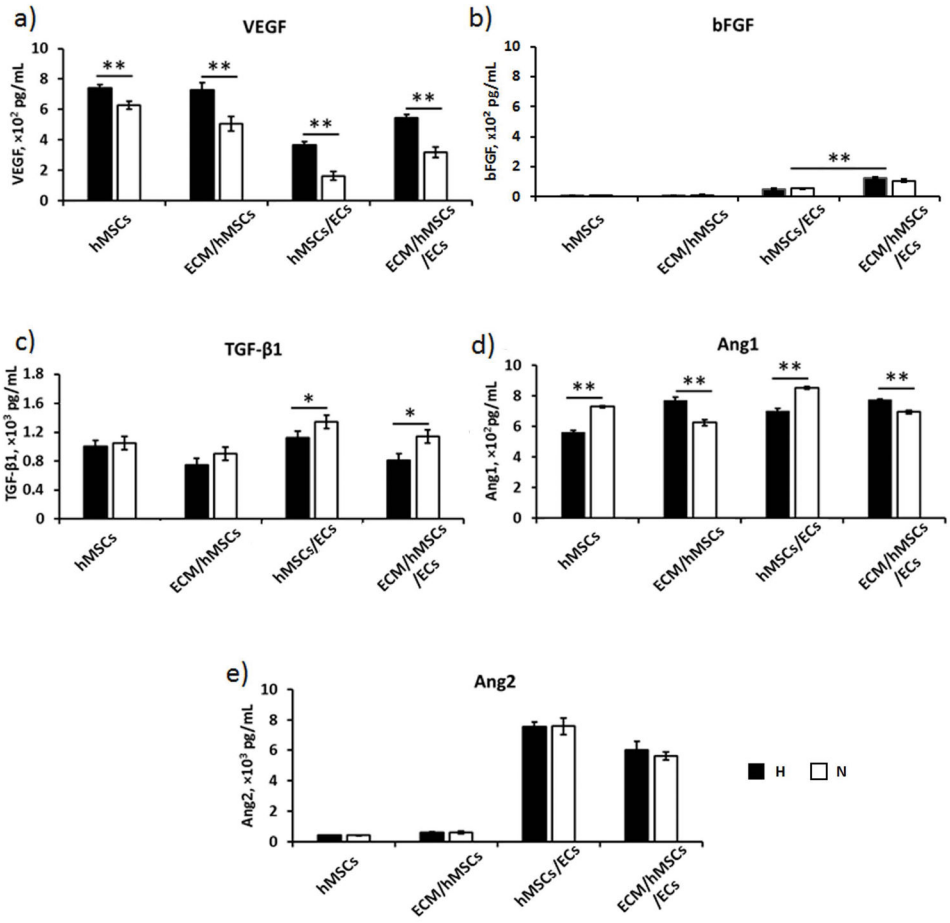

Figure 4.

Secretion of angiogenic growth factors (a) VEGF, (b) bFGF, (c) TGF-β1, (d) Ang-1, and (e) Ang-2 at day 7. The concentrations of VEGF, bFGF, and Ang-1 were increased in H-groups (only when ECM was present), while the TGF-β1 and Ang-1 (ECM absent) decreased in the H-groups. (*$p < 0.05$, **$p < 0.01$)

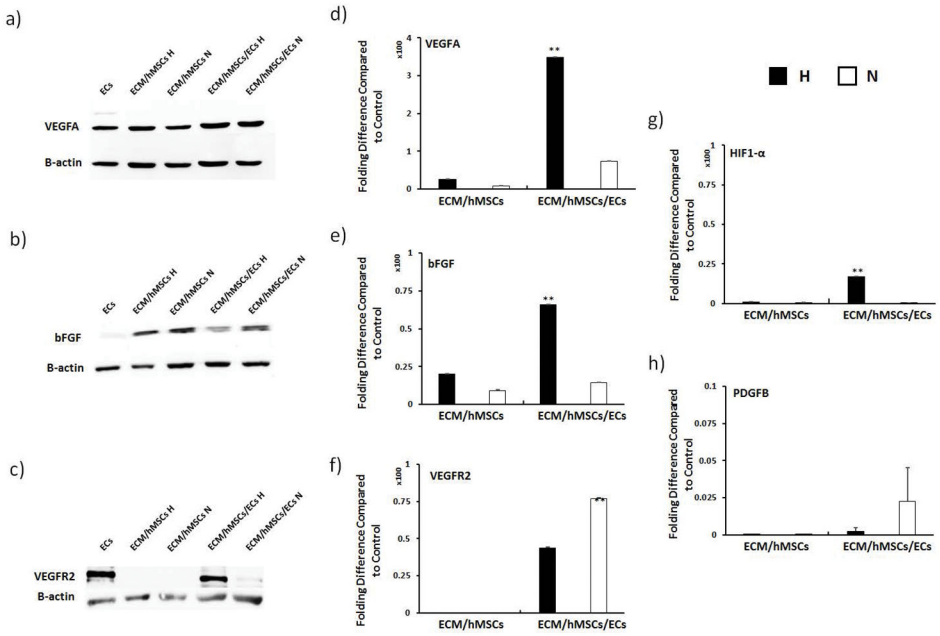

Figure 5.

Effects of hypoxia on angiogenic growth factor secretion (a–c) and gene expression (d–h) on pre-vascularized samples at day 7. The gene expression of VEGFA, bFGF, and HIF-1α were significantly higher in the H-groups. The protein secretion of VEGFR2 was significantly higher in the H-groups. But gene expression of VEGFR2 was lowered at day 7. (**$p < 0.01$)

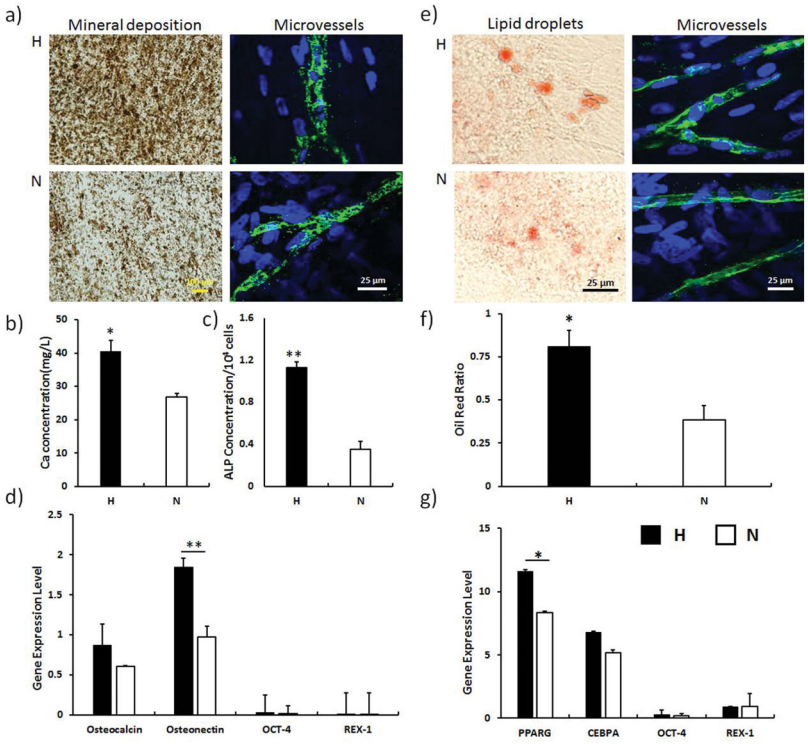

Figure 6.

Osteogenic differentiation (14 days) and adipogenic differentiation (21 days) of hMSCs after vascularization. a) Von Kossa staining of the differentiated groups and undifferentiated control. b) Quantification of ALP activity. c) Quantification of Ca^{2+} concentration. d) Expression of osteogenic and stemness genes. The hypoxia samples showed enhanced ALP activity and calcium deposition as well as higher osteogenic gene expression. e) Oil red O staining of the lipid droplet after the adipogenic differentiation of hMSCs. More lipid droplets were visualized in the H-group. f) Quantification of Oil red O staining. Hypoxia significantly enhanced the oil red ratio. g) Gene expression of adipogenic differentiation genes and stemness genes. Expression of adipogenic genes was enhanced in the hypoxia samples. (*$p < 0.05$, **$p < 0.01$)

Table 1

List of primer sequences

Common Name	Gene ID	Forward Sequence	Reverse Sequence
GAPDH	GAPDH	5′ - ACAGTTGCCATGTAGACC	5′ - TTTTTGGTTGAGCACAGG
OCT-4	POU5F1	5′ - GATCACCCTGGGATATACAC	5′ - GCTTTGCATATCTCCTGAAG
Rex-1	ZFP42	5′ - GAATTCAGACCTAACCATCG	5′ - TGAGCACTACTAGAGTGAAG
VEGFA	VEGFA	5′ - GACCAAAGAAAGATAGAGCAAG	5′ - ATACGCTCCAGGACTTATAC
bFGF	FGF2	5′ - CAAGCAGAAGAGAGAGGAG	5′ - CACTCATCCGTAACACATTTAG
HIF-1α	HIF1A	5′ - TGGAAACGTGTAAAAGGATG	5′ - CTACATGCTAAATCAGAGGG
PDGFB	PDGFB	5′ - TTCAGTTTGTAAAGTCGGTG	5′ - TTTCATTTGGTTTTGTTTTGTG
VEGFR2	KDR	5′ - GTACATAGTTGTCGTTGTAGG	5′ - TCAATCCCCACATTTAGTTC
PPARG	PPARG	5′ - TCATAATGCCATCAGGTTTG	5′ - CTGGTCGATATCACTGGAG
CEBPA	CEBPA	5′ - AGCCTTGTACTGTATG	5′ - AAAATGGTTTAGCAGAG
Osteocalcin	BGLAP	5′ - TTCTTTCCTCTTCCCCTTG	5′ - CCTCTTCTGGAGTTTATTTGG
Osteonectin	SPARC	5′ - AGTATGTGTAACAGGAGGAC	5′ - AATGTTGCTAGTGTGATTGG